ACS Catalysis

Research Article

pubs.acs.org/acscatalysis

Carbon Nanotubes as Activating Tyrosinase Supports for the Selective Synthesis of Catechols

Fabiana Subrizi,[†] Marcello Crucianelli,*[,†] Valentina Grossi,[†] Maurizio Passacantando,[†] Lorenzo Pesci,[‡] and Raffaele Saladino*[,‡]

[†]Department of Physical and Chemical Sciences, University of L'Aquila, Via Vetoio, I-67100 Coppito, AQ, Italy

[‡]Department of Ecology and Biology, University of Tuscia, Largo dell'Università, 01100 Viterbo, VT, Italy

Supporting Information

ABSTRACT: A series of redox catalysts based on the immobilization of tyrosinase on multiwalled carbon nanotubes has been prepared by applying the layer-by-layer principle. The oxidized nanotubes (ox-MWCNTs) were treated with poly(diallyl dimethylammonium chloride) (PDDA) and tyrosinase to yield ox-MWCNTs/PDDA/tyrosinase **I**. Catalysts **II** and **III** have been prepared by increasing the number of layers of PDDA and enzyme, while **IV** was obtained by co-immobilization of tyrosinase with bovine serum albumin (ox-MWCNTs/PDDA/BSA-tyrosinase). Attempts to covalently bind tyrosinase provided weakly active systems. The coating of the enzyme based on the simple layer-by-layer principle has afforded catalysts **I**–**III**, with a range of activity from 21 units/mg (multilayer, **II**) to 66 units/mg (monolayer, **I**), the best system being catalyst **IV** (80 units/mg). The novel catalysts were fully characterized by scanning electron microscopy and atomic force microscopy, showing increased activity with respect to that of the native enzyme. These catalysts were used in the selective synthesis of catechols by oxidation of *meta*- and *para*-substituted phenols in an organic solvent (CH_2Cl_2) as the reaction medium. It is worth noting that immobilized tyrosinase was able to catalyze the oxidation of very hindered phenol derivatives that are slightly reactive with the native enzyme. The increased reactivity can be ascribed to a stabilization of the immobilized tyrosinase. The novel catalysts **I** and **IV** retained their activity for five subsequent reactions, showing a higher stability in organic solvent than under traditional buffer conditions.

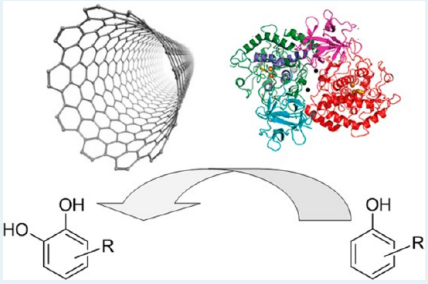

KEYWORDS: *tyrosinase, carbon nanotubes, catechols, biocatalyst, layer by layer, supported enzyme*

INTRODUCTION

Biological conversions using enzymes, being highly specific, commonly require milder reaction conditions than classical chemical catalysis. The poor stability of enzymes, the easy inactivation caused by solvent or mechanical stress, and the high cost of purification are sometimes the main drawbacks of this methodology. To improve their performance and economic viability, enzymes are generally immobilized onto a support. Immobilization can improve the activity and stability, allowing better handling and usage under unconventional operative conditions.[1] The increase in stability can be achieved via multipoint or multisubunit immobilization, generation of a favorable environment, and prevention of intermolecular phenomena.[1] Increased activity is somehow more complex and unexpected, except in certain cases like multimeric proteins, allosteric proteins, and enzymes that suffer conformational changes, or by ensuring prevention of inhibition−inactivation processes.[1] In addition, immobilization leads to an easier separation of the enzyme from the reaction mixture. Tyrosinase is a copper enzyme that catalyzes the hydroxylation of monophenols to *o*-diphenols and *o*-quinones using dioxygen (O_2) as the primary oxidant.[2] This enzyme has been widely studied because of its relevance in several applied areas.[3,4] In a recent work, we described the preparation of heterogeneous catalysts by immobilization of tyrosinase on the epoxy resin Eupergit C250L.[5] These catalysts provided high catalytic efficiency in the synthesis of catechols and DOPA peptides, showing greater storage life, pH stability, and reusability when coated by the layer-by-layer (LbL) procedure. However, some disadvantages have been highlighted, such as the long duration of loading procedures (incubation time of 24 h), the low enzyme loading, and the use of covalent attachment that, although it improves stability and reduces the extent of leaching, could severely damage the structural integrity of the protein. In this study, the choice of carbon nanotubes (CNTs) as a supporting material for tyrosinase was made to improve the previously mentioned approach. These fascinating nanomaterials offer a high surface area for enzyme loading, with the establishment of hydrophobic or electrostatic interaction for a better assembly between the enzyme and support, as well as biocompatibility and mechanical resistance.[6] In the past, most of the efforts toward the development of tyrosinase supported on CNTs have been focused on the exploitation of their electronic properties and electrode kinetics,[7] with the aim of designing biosensors and

Received: September 26, 2013
Revised: January 19, 2014
Published: January 27, 2014

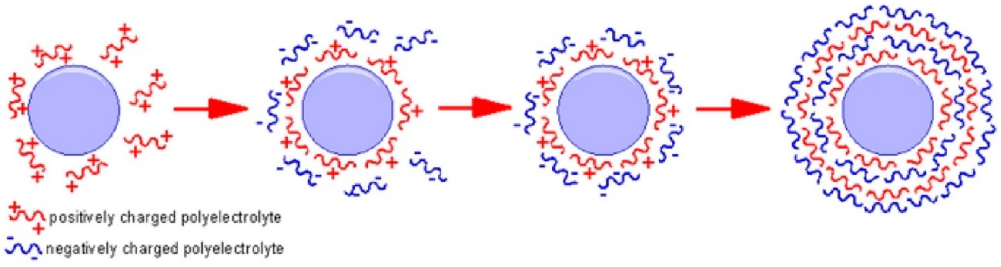

Figure 1. Multishell LbL strategy.

Scheme 1. Synthesis of Catalyst I As Depicted in a Schematic Representation of the Adsorption of Tyrosinase (Tyr) on Ox-MWCNTs/PDDA[a]

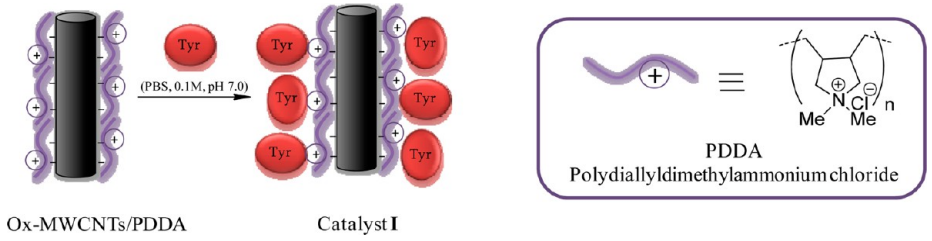

[a]Tyrosinase (negatively charged) is attracted by PDDA (positively charged).

biofuel cells, particularly useful in the detection of phenols[8] or sulfites.[9] On the other hand, their application for synthetic purposes has been largely understudied. Here we describe the preparation and characterization of novel catalysts based on the immobilization of tyrosinase on multiwalled carbon nanotubes (MWCNTs) by the LbL method, focusing our attention on their use as efficient biocatalysts for the synthesis of catechols. This method is based on the consecutive deposition of alternatively charged polyelectrolytes onto the active species (Figure 1).[10] The LbL method is an effective tool for the stabilization of enzymes because polyelectrolyte films can protect proteins from high-molecular mass denaturing agents.[11a−d]

The strategy based upon the formation of a covalent bond by the diimide-activated amidation and the glutaraldehyde-assisted co-immobilization of tyrosinase and bovine serum albumin (BSA) was also exploited, in this work, to anchor tyrosinase on carbon nanotubes. Glutaraldehyde is one of the most widely used reagents in the design of biocatalysts, acting as a useful cross-linker and a versatile tool for enzyme immobilization, by reacting with amino groups of enzymes.[11e] This process may further stabilize multimeric enzymes (like tyrosinase, in this case) by preventing subunit dissociation. Moreover, it can be reasonably assumed that BSA will react via glutaraldehyde with the enzyme, giving a higher stability. Indeed, BSA has been frequently used as a proteic feeder to obtain cross-linked enzyme aggregates (CLEAs).[11f] Catalysts conceived in this way, by combining the unique role of CNTs in supporting the immobilized enzyme and the advantages of enzymatic catalysis in phenol oxidation, would increase the efficiency of the synthetic process with a reduced economic impact.

RESULTS AND DISCUSSION

Preparation of the CNT Support and Optimization of the Immobilization Procedures. Studies were conducted with MWCNTs as supports because of their lower costs and greater commercial availability. MWCNTs show low dispersibility in aqueous solutions, also after prolonged sonication, and this leads to minimization of the available surface for protein immobilization. Hence, before the loading steps, the pristine nanotubes were oxidized under acidic conditions, with the aim of introducing a negative charge onto their surface. The acidic treatment allowed the removal of impurities (residual contamination and amorphous carbons) and the introduction of carboxyl and hydroxyl groups at the ends or sidewall defects of the structure. After prolonged sonication at room temperature with a 3:1 mixture of concentrated sulfuric and nitric acids, the as obtained nanotubes were solubilized in water, and the increase in their solubility was verified by UV−vis spectroscopy (maximal absorbance at 500 nm).[6,12] A linear relationship between absorbance and the concentration of oxidized nanotubes (ox-MWCNTs) was observed: the solutions were stable for more than 1 week (see Figure S1 of the Supporting Information).[12] The ox-MWCNTs were successively treated with a positively charged polyelectrolyte by the LbL technique to facilitate the loading of tyrosinase, negatively charged at the operative pH (7.0; isoelectric point of 4.7−5.0).[13] Commercially available poly(diallyl dimethylammonium chloride) (PDDA) was used as polycation, and the coating was applied.[14,15] Briefly, ox-MWCNTs were treated with PDDA in 0.5 M NaCl, and the suspension was subjected to orbital shaking to yield ox-MWCNTs/PDDA. The 0.5 M NaCl solution was used to optimize the ionic strength of the mixture, helping the dispersion of nanotubes to facilitate the deposition of the polyelectrolyte. Before the deposition of the next layer, the excess PDDA was removed by centrifugation−redispersion cycles. The absence of residual PDDA in the solution is critical to the adsorption of the following layer because a precipitate would form upon mixing with the enzyme. Ziółkowska et al. recently reported a simple method for the determination of the PDDA concentration in solution based on the Bradford procedure.[16] To ensure the complete removal of the polyelectrolyte, UV−vis spectra of each supernatant with Coomassie Brilliant Blue (CBB) were recorded until no evidence of the CBB−PDDA complex was detected. This method, being quantitative, also permits the determination of the amount of PDDA in the solution and, hence, the efficiency of PDDA deposition. Monitoring the absorbance at 595 nm, we

dx.doi.org/10.1021/cs400856e | ACS Catal. 2014, 4, 810−822

found the amount of PDDA adsorbed per milligram of nanotubes was 0.573 mg. In the preparation of catalyst **I** (ox-MWCNTs/PDDA/tyrosinase), the optimal weight ratio between the enzyme and the support was investigated. The ox-MWCNTs/PDDA (1.0 mg) system was treated with different amounts of tyrosinase (0.02−2.00 mg) in sodium phosphate buffer (PBS, 0.1 M, pH 7.0), and the effectiveness of the immobilization was evaluated by analyzing the residual activity in the waste waters (Scheme 1).

Tyrosinase (Tyr) activity was determined by the dopachrome assay[17] following the oxidation of L-tyrosine at 475 nm; the enzyme unit is defined in terms of the increase in absorbance of 10^{-3} unit/min at 25 °C in 0.1 M phosphate buffer (pH 7.0). The activity of immobilized tyrosinase was expressed as the activity unit per milligram of support (eq 1), where U_x is the activity (units) of the immobilized enzyme assayed by the dopachrome method.

$$\text{activity (units/mg)} = U_x/W_{\text{support}} \quad (1)$$

Immobilization and activity yields were evaluated as reported in eqs 2 and 3, respectively.

$$\text{activity yield (\%)} = [U_x/(U_a - U_r)] \times 100 \quad (2)$$

$$\text{immobilization yield (\%)} = [(U_a - U_r)/U_a] \times 100 \quad (3)$$

where U_a is the total activity (units) of the enzyme added to the solution and U_r is the residual activity (units) evaluated by the dopachrome method in the washing solutions. As reported in Table 1, the immobilization yield increased with an increase in the support:enzyme ratio while the activity reached a maximum at a ratio of 5 (Table 1, entry 3). Thus, it appears that there is a critical concentration value beyond which any further immobilization of the enzyme decreases its activity instead of continuing to increase it. The low activity at high enzyme concentrations (Table 1, entry 1) can reasonably be attributed to close packing effects. On the other hand, the possibility that a high enzyme concentration may affect the structure of the polymeric bed, producing a negative effect on the activity, cannot be completely ruled out. The activity yield exhibited a similar behavior.[18] Note that the unsupported enzyme may be successfully immobilized in following batches.

Table 1. Activity Parameters for Catalyst I[a]

entry	support/Tyr (mg/mg)	immobilization yield (%)	activity yield (%)	activity (units/mg)[b]
1	0.5	16	<1	11
2	1	17	11	59
3	5	46	27−34	66
4	10	47	19−24	44
5	15	70	13	23
6	25	73	13	10
7	50	74	6	3

[a]All experiments were conducted in triplicate. Average errors were ~0.1% for immobilization yield and 0.1−0.2% for activity yield and activity. [b]The activity of native tyrosinase, evaluated by the dopachrome method, was 2568 units/mg of enzyme (see ref 25).

Next, experiments were performed using a support:enzyme ratio of 5:1. These optimized conditions would ensure maximal efficiency of the catalyst with minimal enzyme waste. Subsequently, we applied the LbL technique to increase the number of layers of PDDA and enzyme. In particular, catalysts **II** (Figure 2A) and **III** (Figure 2B) were prepared by addition of PDDA and PDDA/Tyr layers, respectively.

These catalysts showed lower activity (21 and 43 units/mg, respectively) than catalyst **I**. Thus, the efficiency of the catalysts is not influenced by the number of layers. A different pattern was observed when the Tyr/PDDA multilayer system was progressively assembled on a quartz slide.[3g] The lower activity observed for catalysts **II** and **III** compared to that of **I** requires a brief comment. In the case of **II**, the addition of the outer layer of PDDA can affect the diffusion of the substrate, inhibiting the interaction with the enzyme. On the other hand, in catalyst **III**, the outer layer is similar to **I**. In this latter case, it is possible to suggest that the second layer of tyrosinase is partially dissolved in PDDA, even if the possibility of an active role of nanotubes (which are redox active and now more distant from the surface of the catalyst) cannot be completely ruled out. The chemical immobilization of tyrosinase on ox-MWCNTs was also performed. The use of a covalent bond to anchor enzymes to carbon nanotubes is well-documented, and we tried to follow this method to increase the stability of the system. The immobilization was achieved using a two-step process through the diimide-activated amidation and employing the optimal support:enzyme ratio. Briefly, ox-MWCNTs were activated by *N*-ethyl-*N*′-(3-dimethylaminopropyl)carbodiimide hydrochloride (EDC) in the presence of *N*-hydroxysuccinimide (NHS), followed by enzyme coupling.[9,19] Despite the high value of protein immobilization (immobilization yield of 52%), a low activity (9.0 units/mg) was obtained: probably, in this case, chemical immobilization had a negative effect on enzyme conformation. With the aim of further improving the efficiency of catalyst **I**, we also investigated the glutaraldehyde-assisted co-immobilization of tyrosinase and BSA.[20] The immobilization efficiency is dependent upon the number of enzyme molecules loaded onto a given surface area. In such situations, given the large surface area of nanotubes, the enzyme strives for the greatest surface coverage, leading to conformational changes that

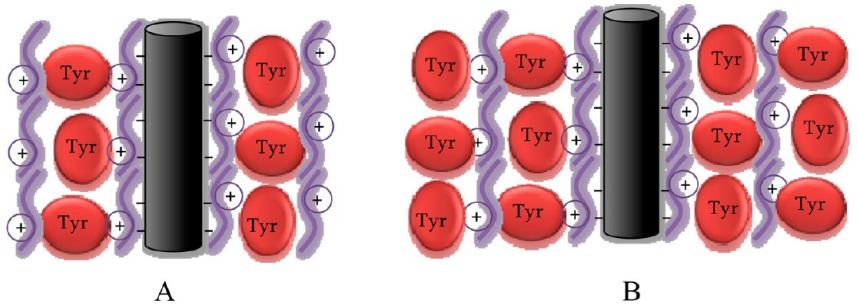

Figure 2. Representations of catalysts **II** (A) and **III** (B).

dx.doi.org/10.1021/cs400856e | *ACS Catal.* 2014, 4, 810−822

Scheme 2. Synthesis of Catalyst IV As Depicted by a Schematic Representation of the BSA-Assisted Co-immobilization of Tyrosinase (Tyr) on ox-MWCNTs

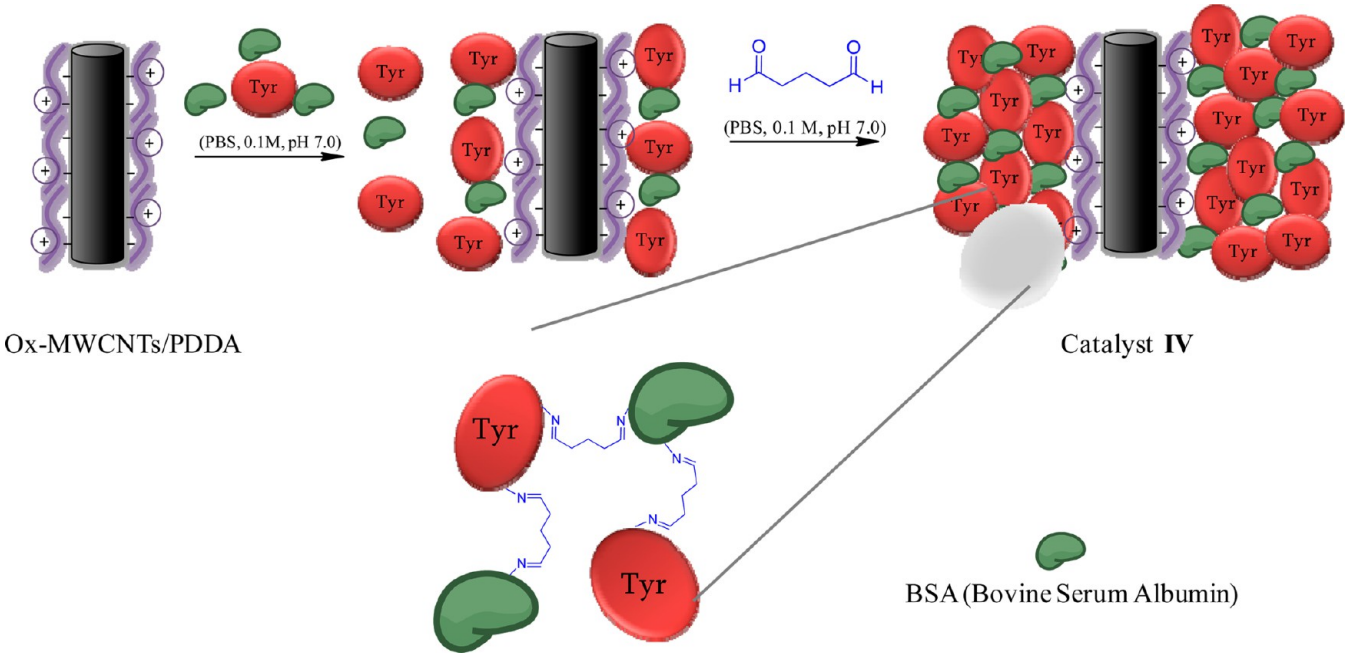

could influence its activity. This effect can be avoided by the addition of an inert protein that reduces the amount of surface area available to the enzyme. BSA, with an isoelectric point close to that of tyrosinase, was the protein selected for this purpose.[21] Glutaraldehyde (GA) was used as the cross-linking agent for the formation of a three-dimensional network "to confine" the enzyme as shown for the catalyst ox-MWCNTs/PDDA/BSA-tyrosinase **IV** (Scheme 2).

Briefly, Tyr and BSA were immobilized on PDDA-coated MWCNTs in the presence of GA following the general procedure reported by Kim et al. for the preparation of Tyr-based sensitive electrochemical immunosensors.[22a] In particular, different amounts of BSA were studied, maintaining the MWCNTs:Tyr ratio of 5:1 (milligrams) already selected for catalyst **I**, and the optimal value of GA concentration [0.5−1.0% (v/v)] previously described in the literature.[3h] The immobilization yield increased when the BSA:Tyr ratio increased to 3:1 and then decreased, suggesting this last value was the optimal one (Table 2, entries 1−4). The activity parameters showed a similar behavior. The 3:1 BSA:Tyr ratio had been previously reported as the optimal value in the preparation of biosensors based on the immobilization of Tyr on MWCNTs in a glassy carbon electrode.[22b]

Table 2. Activity Parameters for Catalyst IV[a]

entry	BSA:Tyr[b]	immobilization yield (%)	activity yield (%)	activity (units/mg)
1	1:1	56	38	68
2	2:1	60	40	71
3	3:1	67	47	80
4	4:1	63	42	73

[a]Support:Tyr ratio of 5:1 (milligrams). [b]Final concentration of GA of 0.5−1.0% (v/v). Note that changes in both activity and immobilization parameters in the range of used GA concentrations [0.5−1.0% (v/v)] were not observed. In accordance with ref 22a, treatment with GA after the removal of the unbound Tyr inhibited the performance of catalyst **IV** (49% of immobilization yield, 36% of activity yield).

The activity and immobilization parameters varied slightly close to the optimal value (see, for example, entries 2 and 4 vs entry 3) in accordance with data previously reported for similar systems.[20] The treatment with GA before the removal of the unbounded proteins allowed the increase in enzyme loading by cross-linking additional tyrosinase and BSA without affecting the activity. Catalyst **IV** was more active than previous systems (80 units/mg), showing a 67% immobilization yield. Among the novel catalysts, **I** and **IV** (the most active) were selected for successive characterizations and applications.

Scanning Electron Microscopy (SEM) and Atomic Force Microscopy (AFM). The topography and morphology of catalysts **I** and **IV** were examined by SEM and AFM to demonstrate the effective polyelectrolyte deposition and enzyme immobilization. The analyses were performed on well-dispersed and separated MWCNTs supported on a silicon substrate (Si). Figure 3 shows the SEM images and the corresponding AFM images[23] of the selected areas of the different samples. MWCNTs well dispersed and separated on Si are shown in Figure 3a. The corresponding AFM image (Figure 3b) shows the detail of a single nanotube immobilized on Si; the white areas, which are higher than the substrate, are drag from the AFM tip during the scanning. The SEM image of ox-MWCNT/PDDA (Figure 3c) showed a cluster of functionalized nanotubes. Only at the cluster edge is it possible to find individual functionalized nanotubes. The AFM morphological study (Figure 3d) allowed the evaluation of the cluster height that is ∼1 μm.

The SEM analysis (Figure 3e) of catalyst **I** showed that the nanotubes with the immobilized enzyme were more dispersed, broken, and shorter than the original MWCNTs. The AFM analysis (Figure 3f) showed the remarkable roughness of the external structure that completely covers the nanotube.

For catalyst **IV**, we obtained a good dispersion of nanotubes onto Si, but after sonication, they appeared to be broken (Figure 3g). The AFM image (Figure 3h) shows small clusters of

dx.doi.org/10.1021/cs400856e | ACS Catal. 2014, 4, 810−822

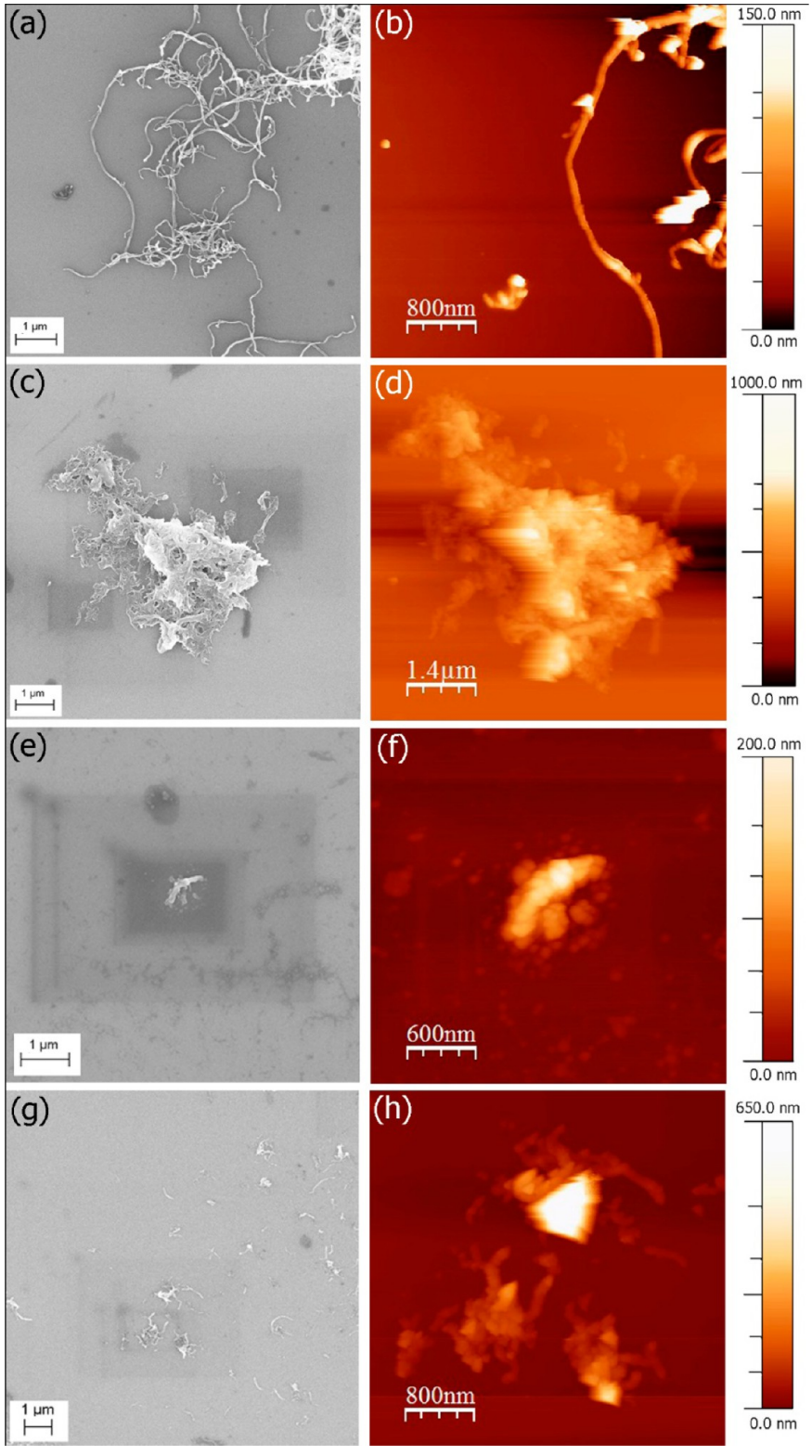

Figure 3. SEM and AFM images of MWCNTs (a and b), ox-MWCNTs/PDDA (c and d), catalyst **I** (e and f), and catalyst **IV** (g and h) deposited on silicon substrates.

nanotubes, and individual functionalized nanotubes are clearly visible.

Figure 4 reports the high-resolution AFM images of individual MWCNTs and the related image profiles for selected directions (line in Figure 4a). The nanotube surface appears to be smooth, and the maximal height (h) and width at half-height (d), evaluated by a profile analysis (Figure 4c), were 39.0 ± 0.5 and 53 ± 2 nm, respectively. The width of the nanotube has been estimated at half-height and not at the bottom to reduce the size of errors resulting from effects of tip convolution.

High-resolution AFM images of ox-MWCNT/PDDA at the same scale (300 nm × 300 nm) of the previous sample are

dx.doi.org/10.1021/cs400856e | *ACS Catal.* 2014, 4, 810−822

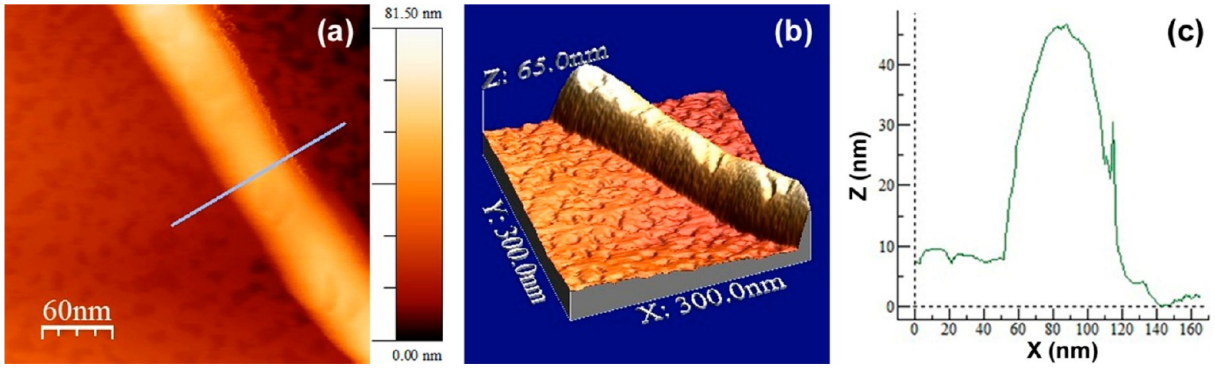

Figure 4. High-resolution AFM images for MWCNTs: (a) bidimensional and (b) tridimensional analyses. The line in panel a indicates the section that was further analyzed for the image profile (c).

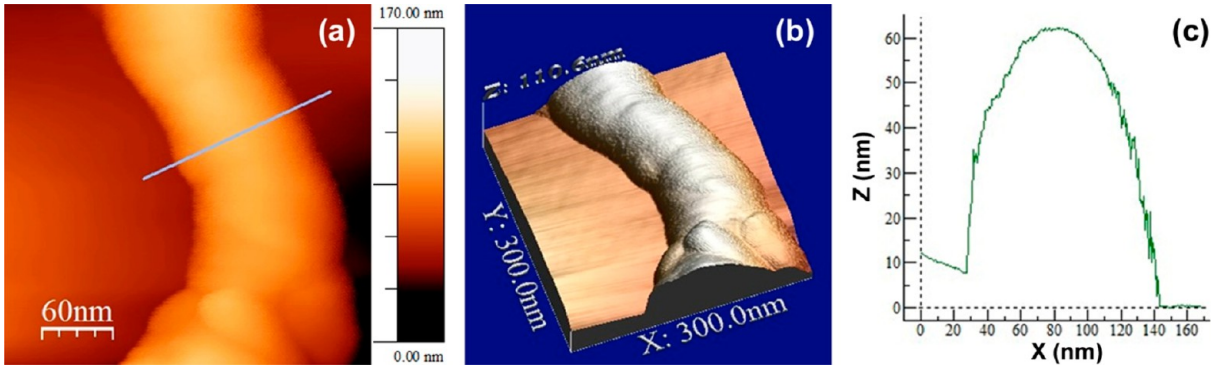

Figure 5. High-resolution AFM images for ox-MWCNT/PDDA: (a) bidimensional and (b) tridimensional analyses. The line in panel a indicates the section that was further analyzed for the image profile (c).

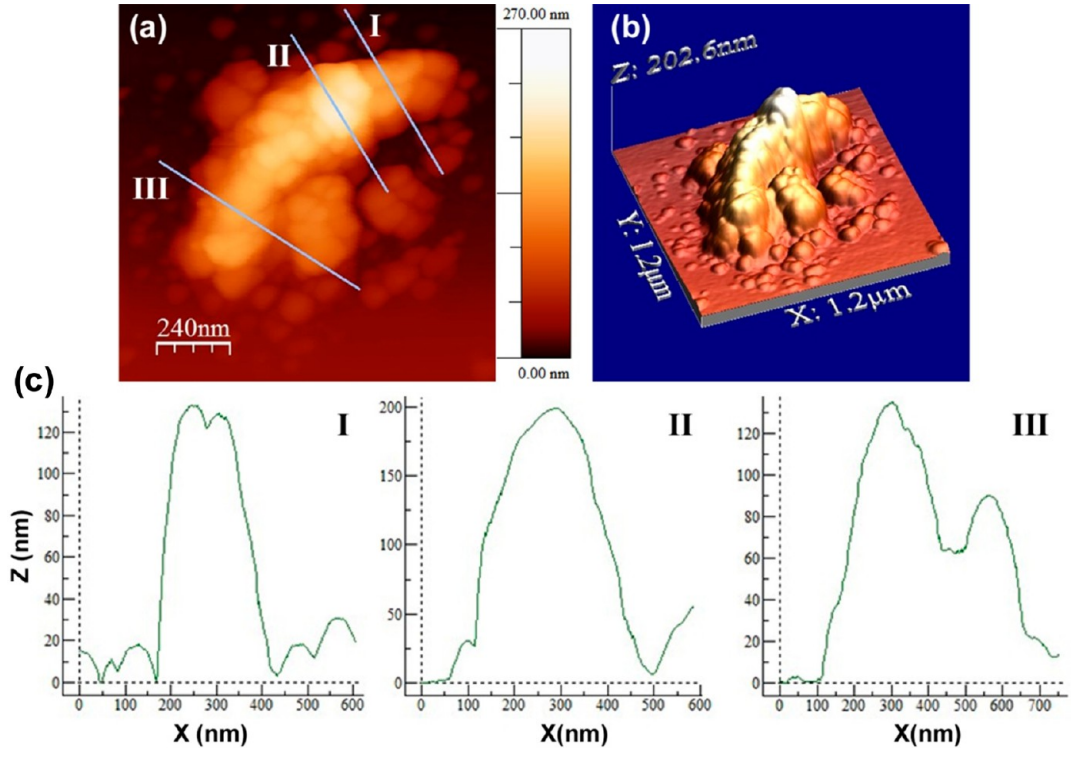

Figure 6. High-resolution AFM images for catalyst **I**: (a) bidimensional and (b) tridimensional analyses. Lines I–III in panel a indicate the sections that were further analyzed for the image profiles (c).

reported in Figure 5. Although the surface is smooth, h and d were 60.5 ± 0.5 and 90 ± 2 nm, respectively (Figure 5c). The dimensions of the system are doubled, confirming that an external shell covers the nanotube.

dx.doi.org/10.1021/cs400856e | *ACS Catal.* 2014, 4, 810–822

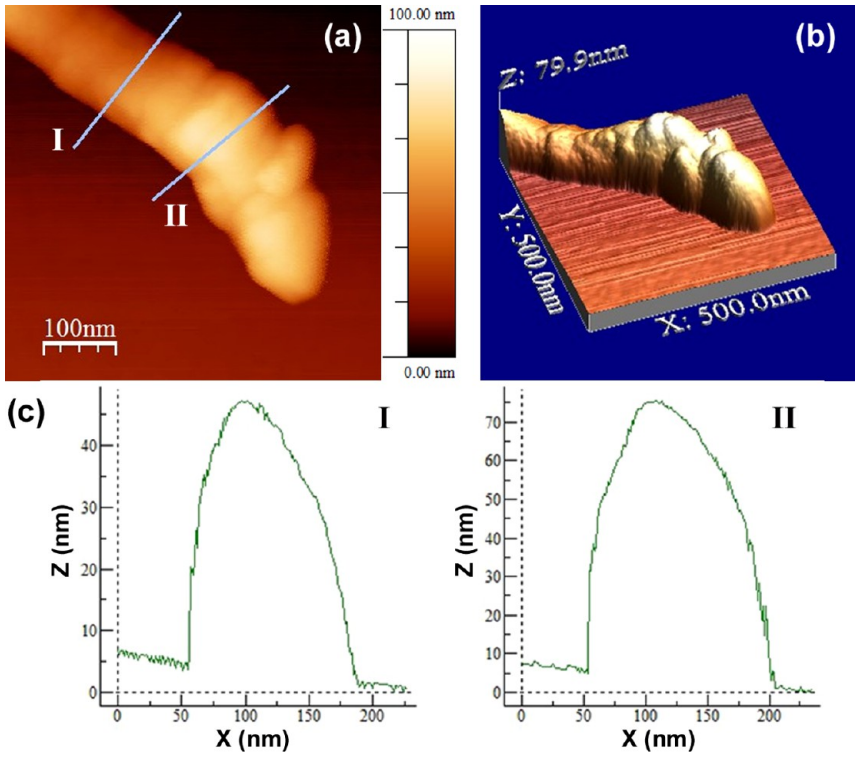

Figure 7. High-resolution AFM images for catalyst **IV**: (a) bidimensional and (b) tridimensional analyses. Lines I and II in panel a indicate the sections that were further analyzed for the image profiles (c).

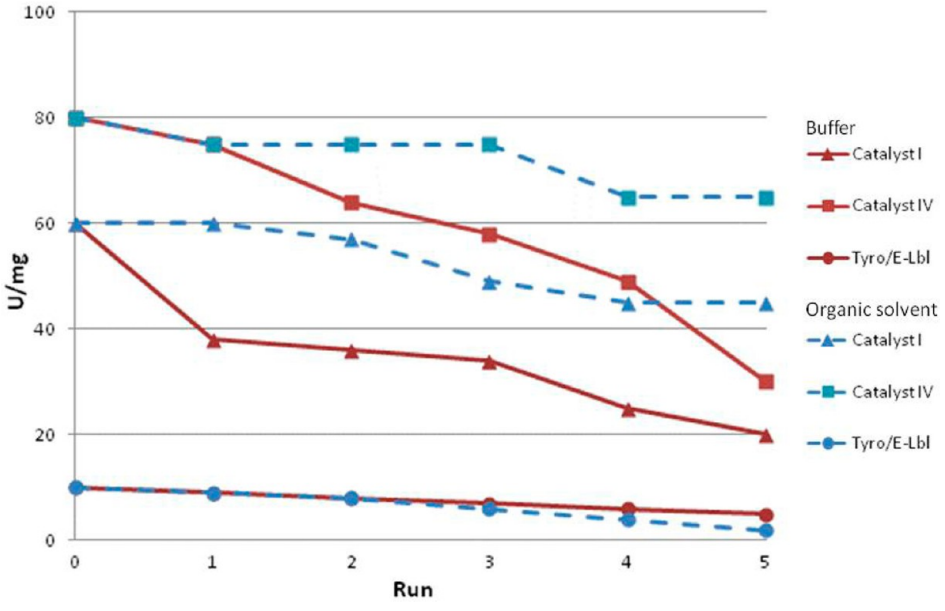

Figure 8. Activity of catalysts **I** and **IV** vs the number of runs, in buffer and in organic solvent.

The AFM analysis of catalyst **I** (Figure 6) showed the remarkable roughness and the presence of external "lumps" that can be attributed to tyrosinase, which completely covers the nanotube. To estimate the size of both the nanotube and the lumps, three different image profiles were performed (Figure 6c). From profile II, the maximal h of the whole structure is 199.0 ± 0.5 nm and the d is 259 ± 2 nm. From profiles I and III, we obtained the lump d that ranges from 62 ± 2 to 80 ± 2 nm.

The AFM image (Figure 6b) shows small clusters where individual functionalized nanotubes are clearly visible. Finally, high-resolution AFM images of catalyst **IV** (Figure 7) show a lower roughness and fewer lumps than catalyst **I**. The smoother surface can be explained by suggesting that BSA occupies interstitial sites between tyrosinase molecules. Maximal heights and widths of 46.0 ± 0.5 and 101 ± 2 nm, respectively, for profile I and 70.0 ± 0.5 and 126 ± 2 nm, respectively, for profile II (Figure 7c) were obtained.

Reusability Properties and Storage Stability. The reusability properties of catalysts **I** and **IV** were evaluated in both buffer and organic solvent, performing five consecutive

dx.doi.org/10.1021/cs400856e | *ACS Catal.* 2014, 4, 810−822

oxidations of L-tyrosine in 0.1 M PBS (pH 7.0) (Figure 8, red line) and *p*-cresol in CH_2Cl_2 and buffer (Figure 8, blue line), respectively. Several advantages can be obtained using enzymes in organic solvents, such as the enhanced solubility of hydrophobic substrates, reduced side reactions, enhancement of catalyst performance, and simple recovery from the reaction mixture.[24] Previously published data from our laboratory showed that CH_2Cl_2 plays a benign role in the synthesis of catechols.[25] A minimal amount of phosphate buffer was also used to disperse the catalysts, because water is fundamental for the correct folding of the enzyme and consequently for its proper functionality. The oxidations were followed at 475 nm (in buffer) or 389 nm (in CH_2Cl_2 and buffer), and after the absorbance plateau had been reached, the immobilized enzyme was recovered by simple centrifugation, washed, and reused with a fresh substrate. Data referring to tyrosinase immobilized on Eupergit (Tyro/E-LbL) are shown in Figure 8 as ref 25. As a general trend, the reusability of catalysts **I** and **IV** was higher in organic solvent than in buffer. The organic medium strongly improved the stability and efficiency of the catalysts, and only a minimal loss of activity was observed during the first five runs, for catalysts **I** and **IV**. Irrespective of experimental conditions, catalyst **IV** was more reactive than **I**. This result may be due to a more rigid enzyme structure in **IV** that can resist conformational changes that could affect activity.[26] The T_{50} values for **I** and **IV** in buffer (defined as the run number at which the catalyst activity is reduced to 50%) were found to be 3 and 4, respectively [T_{50} was calculated by linear regression of the percentage of activity vs run plot (see Figures S2 and S3 of the Supporting Information)]. In organic solvent, the T_{50} values of **I** and **IV** were 8 and 12, respectively. The novel catalysts exhibited better performance with respect to the Tyro/E-LbL system.[25]

The reusability experiments showed different behaviors of catalysts **I** and **IV** in the different solvents. In particular, the lower T_{50} values for catalysts **I** and **IV** in buffer can be justified by invoking the stronger tendency of the *o*-quinones (formed in the oxidation of *o*-diphenols) to undergo a sequence of non-enzymatic reactions, in this medium, leading to synthetic melanin as a final product. These insoluble polymers can precipitate and be strongly adsorbed on the functionalized nanotubes that cannot be reused. This phenomenon is particularly evident in buffer, where the polymerization process is favored.[3g]

Further, the stability of the new systems, namely, native tyrosinase and catalysts **I** and **IV**, was evaluated by storing the catalysts in PBS at 4 °C for 20 days. The activity was measured at specific times at room temperature by the oxidation of *p*-cresol in the mixed organic medium (PBS and CH_2Cl_2) (Figure 9).

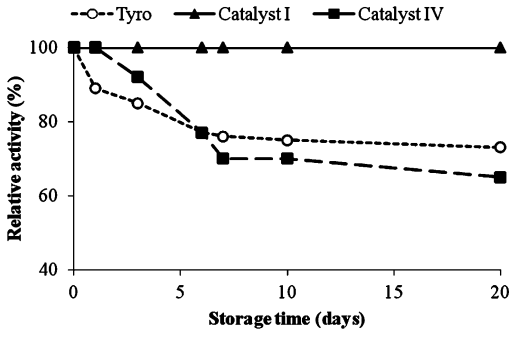

Figure 9. Storage stability of native tyrosinase and catalysts **I** and **IV** at 4 °C.

While the native enzyme and catalyst **IV** showed a slight decrease of activity in the first 7 days, thereby reaching a constant value of ∼70% of residual activity, catalyst **I** retained the full activity for up to 20 days. With respect to the storage stability of **IV**, Bakir et al.[27] described a loss of activity, for cross-linked immobilized tyrosinase in the presence of BSA, in the range of 10−20% after 20 days (depending on the purity of the enzyme). These data are comparable with the results observed, in our case, for catalyst **IV**. Thus, the maintenance of the catalytic activity for successive reactions shown above, along with data on their storage stability, confirms the excellent general behavior in terms of the stability of the prepared catalysts **I** and **IV**.

Kinetic Analyses. Kinetic parameters for native tyrosinase and selected catalyst **I** were evaluated in CH_2Cl_2 and PBS, using *p*-cresol as the substrate. The initial reaction rates were measured at substrate concentrations ranging from 1.0 to 20 mM at 25 °C. Because catechol dehydrogenation is reported to follow Michaelis−Menten kinetics, benzoquinone formation was measured at 389 nm. Kinetic constants were evaluated by using different linear regression equations [Lineweaver−Burk, Eadie−Hofstee, and Hanes (Figures S4−S6, respectively, of the Supporting Information) and a nonlinear regression plot (Figure S7 of the Supporting Information). The Hanes plot (Figure S6 of the Supporting Information) provided excellent correlation values without the necessity of discarding any point. From a comparison between the linear regression and nonlinear regression plot analyses, we can observe how the Hanes (mainly) and Eadie−Hofstee (to a lesser extent) plots, respectively, gave the best estimations while the Lineweaver−Burk plot has afforded under- or overestimated values (compare Figures S4−S6 of the Supporting Information).

The kinetic parameters (K_m, V_{max}, and K_{cat}) for the native enzyme and catalyst **I** are listed in Table 3.

Table 3. Kinetic Parameters for Native Tyrosinase (Tyr) and Catalyst I[a]

	K_m (mM)		$V_{max} \times 10^4$ (ΔAbs min^{-1} μg of enzyme^{-1})		K_{cat} (min^{-1})	
plot	Tyr	catalyst I	Tyr	catalyst I	Tyr	catalyst I
Lineweaver−Burk	3.92	7.68	49.3	56.1	1310	1683
Hanes	2.52	9.91	43	63	1287	1891
Eadie−Hofstee	2.82	8.12	44	58	1330	1732
nonlinear regression	2.9	10	44	63	1318	1882

[a] K_{cat} is defined as v_{max} (Δabsorbance per minute)/[Tyr] (micromoles per milliliter). All experiments were conducted in triplicate using free and immobilized tyrosinase. Average errors in kinetic parameters were 2−4% for K_m and 1−3% for V_{max}.

As a general trend, the immobilized enzyme (catalyst **I**) showed the highest K_m, probably because of the enzyme conformational changes and mass transfer limitations (Table 3). Irrespective of the regression plot used, catalyst **I** showed a higher rate and a higher turnover number than the native enzyme, thus suggesting the stabilizing effect of the nanotubes.[28] Experimental values were also fit using nonlinear regression procedures like GraphPad Prism6: this method permits us to obtain standard deviations of the kinetic parameters and to evaluate the reliability of the previously reported regression plots (Figure S7 of the Supporting Information).

dx.doi.org/10.1021/cs400856e | ACS Catal. 2014, 4, 810−822

Scheme 3. Oxidation of Phenols[a]

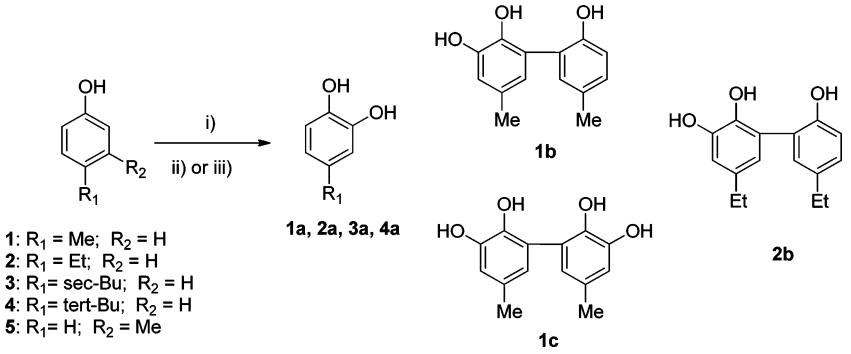

[a](i) Tyro-based catalysts, O_2; (ii) CH_2Cl_2 and buffer; (iii) phosphate buffer.

Table 4. Oxidation of Phenols 1−5 with Native Tyrosinase and Catalysts I and IV in Buffer or CH_2Cl_2 with PBS

entry[a]	catalyst	solvent	substrate	product(s)	conversion (%)	yield (%)[d]
1[b]	tyrosinase	buffer/AA[c]	**1**	**1a**	98	13
2[b]	**I**	buffer/AA[c]	**1**	**1a**	99	6
3[b]	**IV**	buffer/AA[c]	**1**	**1a**	99	6
4	tyrosinase	CH_2Cl_2/buffer	**1**	**1a** [**1b**] {**1c**}	93	54 [4] {14}
5	**I**	CH_2Cl_2/buffer	**1**	**1a** [**1b**] {**1c**}	96	78 [8] {9}
6	**IV**	CH_2Cl_2/buffer	**1**	**1a** [**1b**] {**1c**}	98	82 [4] {3}
7	tyrosinase	CH_2Cl_2/buffer	**2**	**2a** [**2b**]	55	42 [13]
8	**I**	CH_2Cl_2/buffer	**2**	**2a**	80	80
9	**IV**	CH_2Cl_2/buffer	**2**	**2a**	85	85
10	tyrosinase	CH_2Cl_2/buffer	**3**	**3a**	9	<4
11	**I**	CH_2Cl_2/buffer	**3**	**3a**	22	22
12	**IV**	CH_2Cl_2/buffer	**3**	**3a**	25	24
13	tyrosinase	CH_2Cl_2/buffer	**4**	**4a**	8	<5
14	**I**	CH_2Cl_2/buffer	**4**	**4a**	21	21
15	**IV**	CH_2Cl_2/buffer	**4**	**4a**	34	34
16	tyrosinase	CH_2Cl_2/buffer	**5**	**1a** [**1b**]	42	35 [7]
17	**I**	CH_2Cl_2/buffer	**5**	**1a**	35	33
18	**IV**	CH_2Cl_2/buffer	**5**	**1a**	39	39

[a]Reaction conditions: native or immobilized tyrosinase (240 units) in PBS (275 μL), 0.05 mmol of substrate, CH_2Cl_2 (2.5 mL) at 25 °C. All experiments were conducted in triplicate. [b]Solvent of 0.1 M phosphate buffer (pH 7.0). [c]AA, ascorbic acid. [d]The average error in the yield was 0.3%.

Oxidation of Phenols. The synthetic versatility of catalysts **I** and **IV** was evaluated in the oxidation of a panel of selected phenols (**1−5** in Scheme 3) to the corresponding catechol derivatives. Catechols are characterized by several biological activities and are well recognized as antioxidant compounds.[29] The potential of tyrosinase in the synthesis of catechols has received a great degree of attention because they are difficult to obtain under environmentally friendly conditions by means of traditional chemical procedures.[4d,30] The application of tyrosinase in buffer is partially limited because of the formation of reactive *o*-quinones that can covalently bind to the enzyme or polymerize producing brown pigments. For this reason, the oxidation of *p*-cresol **1** was initially performed in the presence of ascorbic acid (AA) that acts as an internal reducing agent.[5] As a general procedure, phenol, native or immobilized tyrosinase (240 units), and AA (1.5 equiv) in a buffer (PBS, 0.1 M, pH 7.0) solution (5.0 mL) were vigorously stirred at room temperature, under a dioxygen atmosphere (O_2), according to a procedure previously reported by our laboratory.[25] Under these conditions, catalysts **I** and **IV** behaved like the native enzyme, showing excellent substrate conversions but only low yields in the desired catechol **1a** (Table 4, entries 1−3).

The low mass balance value observed for the transformation was probably caused by the formation of products of further oxidation and/or of polymeric material not isolated under our experimental conditions. Better results were obtained in organic medium. The substrate in CH_2Cl_2 was treated, at 25 °C, with native or immobilized tyrosinase (240 units) in the presence of the appropriate amount of PBS, thus ensuring the minimal amount of hydration water for the proper functioning of the enzyme. Under these experimental conditions, catalysts **I** and **IV** were more active than the native enzyme, affording **1a** in high yield and conversion of substrate (Table 4, entries 4−6). Dimers **1b** and **1c**, characterized by the formation of the C−C bond between two phenol units, were also detected in very small amounts (Scheme 3 and Table 4, entries 4−6). The blank test performed under conditions similar to those described above showed the absence of any type of reactivity when the support ox-MWCNT was used, without the enzyme, for the oxidation of *p*-cresol **1**, thus confirming its neutral role. The effectiveness of **I** and **IV** in CH_2Cl_2 and buffer was further confirmed with more hindered *para*-substituted phenols **2−4**. Again, in the oxidation of 4-ethyl phenol **2**, catalysts **I** and **IV** were more reactive than native tyrosinase, catechol **2a** being detected in high yields and conversions of substrate (Table 4, entries 7−9). It is noteworthy

dx.doi.org/10.1021/cs400856e | ACS Catal. 2014, 4, 810−822

that no dimers were produced with immobilized tyrosinase in entries 8 and 9. Catalysts **I** and **IV** were highly active also in the oxidation of hindered 4-*s*-butyl phenol **3** and 4-*tert*-butyl phenol **4**, because these substrates were not converted by native tyrosinase under the experimental conditions tested. Catechols **3a** and **4a** were obtained in 22−24 and 21−34% yields, respectively (Table 4, entries 10−15). Previous studies showed the possibility of slightly oxidizing **3** and **4** with native tyrosinase in CH_2Cl_2 and buffer using only 600−1400 units of the enzyme.[19] As a general trend, the efficiency of catalysts decreased with an increase in the steric hindrance of the *para* substituent. These results are in accordance with previously reported data on the low reactivity of bulky phenols with tyrosinase in organic medium, because of the reduced conformational flexibility of the enzyme in a hydrophobic solvent.[31] Catalysts **I** and **IV** were also active in the oxidation of 3-methyl phenol (*m*-cresol) **5** as a selected example of a *meta*-substituted substrate, and **1a** was obtained in 33 and 39% yields, respectively [conversion of substrate in the range of 35−39% (Table 4, entries 16−18)]. Irrespective of the experimental conditions, **IV** was more reactive than **I**, confirming the positive role of BSA in the immobilization of tyrosinase. From a comparative point of view, if we refer to catechol **1a** as the main reaction product, the yields obtained with catalysts **I** and **IV** are comparable and, in some cases, slightly larger than those previously obtained by us with the reference catalyst (Tyro/E-LbL),[25] in spite of the remarkable fact that in catalysts **I** and **IV** a smaller amount of enzyme has been immobilized per weight of support.

CONCLUSIONS

The activity and efficiency of tyrosinase immobilized on carbon nanotubes vary significantly depending on the applied immobilization procedure. The coating of the enzyme based on the LbL principle has afforded the best catalysts since the deposition of the first layer of enzyme. The activity of catalyst **I** reached a maximum at a support:tyrosinase ratio of 5, and it was found to decrease in the presence of a high enzyme concentration, probably because of close packing effects. The deposition of the second PDDA layer decreased the activity, although it started to increase again with a further increase in the number of enzyme layers. In the glutaraldehyde-assisted immobilization procedure, the presence of BSA as protein spacer leads to the more active catalyst **IV**, confirming the favorable role of the protein to avoid steric effects and conformational changes in tyrosinase. In accordance with the literature, the chemical linkage was the less efficient procedure. The new catalysts were more active than previously described heterogeneous systems based on the immobilization of tyrosinase on epoxy resin Eupergit or on His entrapment in a matrix of chitosan.[3h] From a kinetic point of view, the immobilized enzyme showed higher rates and turnover numbers than native tyrosinase. With regard to concerns about stability, catalysts **I** and **IV** retained their activity for more subsequent reactions, showing a higher stability in organic solvent than in buffer. The catalytic performance in the oxidation of phenols to catechols deserves special attention. In fact, catalysts **I** and **IV** were more efficient than the native enzyme in affording catechols **1a**−**4a** in high yield and conversion of substrate. The oxidation in organic medium was the only synthetically useful procedure, because in buffer the products of overoxidation were obtained even in the presence of ascorbic acid as an internal reducing agent. This was particularly evident with bulky substituents, such as 4-*s*-butyl phenol **3** and 4-*tert*-butyl phenol **4**, only oxidized by the immobilized tyrosinase. The greater efficiency of the two biocatalysts probably depends on several factors, including the stabilization of the enzyme by nanotubes and the poor formation of polyphenols as side products that can precipitate on the nanotube inhibiting the tyrosinase activity.[3g] Furthermore, a possible synergic effect of the support in the oxidation cannot be completely ruled out. Recently, Zhong and co-workers showed that oxidized carbon nanotubes are redox active species that can cooperate during the oxidation.[28] They could be themselves the primary oxidant and also could accelerate the reaction of O_2 by energetically favorable absorption processes on the surface (ΔH = −16.3 kcal/mol).[32] These effects were directly related to an increase in peroxidase activity using nanotubes as mediators of oxidation. The possibility of a similar effect in the case of tyrosinase can in part justify the improved reactivity of our catalysts in the oxidation of sterically congested substrates. The active redox role of nanotubes can also explain the observed decrease in activity of catalysts **II** and **III** with an increase in the number of layers with respect to **I**, leading to the hypothesis of a reduction of the synergic effect with an increase in the distance of the enzyme from the support. The high activities of catalysts **I** and **IV** open new stimulating entries for novel oxidation processes of hindered phenols based on tyrosinase.

EXPERIMENTAL SECTION

Reagents and Materials. Multiwalled carbon nanotubes (MWCNTs), mushroom tyrosinase from *Agaricus bisporus* (T-3824, multimeric enzyme with H_2L_2-type structure),[33] BSA, dichloromethane (CH_2Cl_2), ethyl acetate (EtOAc), hexane (Hex), sodium dithionite ($Na_2S_2O_4$), anhydrous sodium sulfate (Na_2SO_4), dodecane, pyridine, hexamethyldisilazane (HMDS), trimethylchlorosilane (TMCS), glutaraldehyde (GA), PDDA, L-tyrosine, and phenols **1**−**5** were purchased from Sigma-Aldrich. All spectrophotometric measurements were taken with a Varian Cary50 UV−vis spectrophotometer equipped with a Peltier thermostated single-cell holder. Dichloromethane was dried on anhydrous sodium sulfate prior to use. All experiments were conducted in triplicate using native and immobilized tyrosinase in the dichloromethane/buffer system and in an aqueous medium. Sodium phosphate buffer (PBS, 0.1 M, pH 7.0) is a solution containing NaH_2PO_4 and Na_2HPO_4 in Milli-Q water; no NaCl is present. This buffer solution was used at pH 7.0 and 0.1 M unless differently specified.

Preparation of Catalysts I−IV. Multiwalled carbon nanotubes (>95% pure, inner diameter of 5−10 nm, outer diameter of 10−30 nm, and length of 0.5−50 μm) were treated with a concentrated sulfuric acid (98%)/nitric acid (65%) mixture [3:1 (v/v)] in a sonication bath for 4 h. The resulting solution was diluted with deionized water and extensively washed by consecutive sonication−centrifugation steps until the pH became neutral. The oxidized nanotubes (ox-MWCNTs) were lyophilized and stored at room temperature as a dry powder.

Coating of MWCNTs with a PDDA Solution. PDDA (2.0 mg) and ox-MWCNTs (1.0 mg) were dispersed in 0.5 M NaCl (2.0 mL) and subjected to sonication for 5 min to give a stable black suspension. After being shaken at 170 rpm for 20 min, the mixture was centrifuged (6000 rpm for 20 min), and the composite was washed with Milli-Q water to remove the residual polyelectrolyte. The absence of a polyelectrolyte in the solution was confirmed by the Bradford method.[16,34]

Preparation of Catalyst I.[35] Tyrosinase was adsorbed on the first polycation layer by incubating the PDDA-coated ox-MWCNTs (1.0 mg) with different amounts of the enzyme

dx.doi.org/10.1021/cs400856e | ACS Catal. 2014, 4, 810−822

(ranging from 2.0 to 0.02 mg) in PBS (0.1 M, pH 7.0) in an orbital shaker at room temperature (40 min at 150 rpm). After the mixture had been shaken, the excess enzyme was removed by centrifugation (6000 rpm × 20 min) and the supernatant was used for immobilization and activity yield calculations. The complex was washed several times with PBS to ensure the complete removal of the unbound enzyme. The absence of tyrosinase in the washing waters was confirmed by both the activity assay and the Bradford method.

*Preparation of Catalysts **II** and **III**.* To reduce the possibility of tyrosinase desorption, a final layer of PDDA (catalyst **II**) and a further layer of tyrosinase (catalyst **III**) were added on **I** following the reported general procedure.

*Preparation of Catalyst **IV**.*[22] Tyrosinase (60 μL, 3.4 mg/mL) and BSA (300 μL, 2.0 mg/mL) were added to a suspension of the PDDA-coated MWCNTs (1.0 mg) in PBS (280 μL). After the mixture had been shaken for 30 min, 2.5% glutaraldehyde (GA) was added to reach a final volume of 800 μL and the mixture was shaken again at room temperature for 30 min and then at 4 °C overnight. Subsequently, the black suspension was centrifuged (6000 rpm × 20 min) to remove the supernatant containing the excess enzyme and GA. The supernatant was used both for immobilization and activity yield calculations. The catalyst was finally treated with 1.5 mL of 0.1 M Tris-HCl buffer (pH 7.2) while being shaken for 1 h at 4 °C (to cap unreacted aldehyde groups) and centrifuged and the supernatant removed. The conjugate sample was washed several times with PBS to ensure the complete removal of the unbound enzyme, and the absence of tyrosinase, in the washing waters, was confirmed by both the activity assay and the Bradford method.

Chemical Attachment of Tyrosinase. To a suspension of nanotubes (1 mg/mL) in 2-(*N*-morpholino)ethanesulfonic acid (MES) buffer (50 mM, pH 6.2) was added *N*-hydroxysuccinimide (NHS) (1 mL, 400 mM in MES buffer). After sonication for 30 min, 1 mL of fresh *N*-ethyl-*N*′-(3-dimethylaminopropyl)-carbodiimide hydrochloride (EDC) in MES buffer (20 mM) was added quickly, and the mixture was stirred at room temperature for 30 min. The activated nanotube solution was then centrifuged at 6000 rpm for 20 min and washed three times with the buffer to remove excess EDC and NHS. A solution containing tyrosinase (0.2 mg in PBS) was added to the activated nanotubes, and the dispersion was shaken at 200 rpm during the conjugation of the enzyme. Unbound tyrosinase was removed by consecutive centrifugation and washing steps.

Determination of the Activity of the Native and Immobilized Enzyme. The activity of the native and immobilized enzyme was determined by measuring the tyrosinase-catalyzed oxidation of L-tyrosine (L-Tyr). The reaction was started by adding the substrate to the solution containing the appropriate amounts of native enzyme or catalysts **I**–**IV** in PBS under magnetic stirring. The initial rates were measured as linear increases in the optical density at 475 nm, due to dopachrome formation. One unit of enzyme activity was defined as the increase in absorbance of 0.001 per minute at pH 7 and 25 °C in a 3.0 mL reaction cuvette containing 0.83 mM L-tyrosine and 67 mM PBS (pH 7.0). Spectrophotometric data were analyzed with Cary WinUV. All experiments were conducted in triplicate using free and immobilized tyrosinase.

SEM and AFM Characterization of Catalysts. The surface morphology of the samples has been studied by SEM analysis, making use of a Zeiss LEO 1530 apparatus equipped with a field emission electron gun, while AFM was conducted with a Digital Dimension D5000 instrument with a Nanoscope IV controller, using commercial silicon tips (frequency range of 51–94 kHz) scanned by means of a Veeco Nanoman closed loop XY head. For the SEM and AFM analysis, different solutions of the samples were prepared. In particular, MWCNT and ox-MWCNTs/PDDA samples were dispersed in pure ethanol and catalysts **I** and **IV** in Milli-Q water, to prevent enzyme denaturation. All the solutions were sonicated for 5 min at room temperature, and a drop of each solution was taken and deposited onto silicon substrates (Si). At the end, the obtained samples deposited on Si were subjected to annealing at 50 °C to quickly evaporate the solvent (ethanol or water).

Determination of the Kinetic Constants. The catalytic properties of native and immobilized tyrosinase were determined in the organic solvent by measuring the initial rates of the reaction with the substrate at 25 °C. The reactions were conducted by using different concentrations of *p*-cresol **1**, ranging from 2 to 18 mM. The appropriate amount of **1** was dissolved in DCM (2.5 mL), and free or immobilized tyrosinase in the optimal aqueous amount (275 μL of PBS) was added. The reaction mixture was stirred for 30 min. Sampling was performed every 6.0 min, the absorbance at 389 nm (due to *o*-quinone) measured, and the sample returned to the flask as rapidly as possible. One unit of enzyme activity was defined as the increase in absorbance of 0.001 at 389 nm and 25 °C in CH_2Cl_2 and 0.1 M PBS (pH 7.0). K_m and V_{max} values were calculated by plotting data in Lineweaver–Burk, Hanes, Eadie–Hofstee, and nonlinear regression plots. All experiments were conducted in triplicate using native and immobilized tyrosinase.

Storage Stability. The storage stability of native and immobilized tyrosinase was estimated by measuring enzyme activity at specific time intervals (0–20 days) and at room temperature in organic medium. The catalysts were stored in PBS (2.0 mg/mL) at 4 °C, and at each time point, an appropriate amount was added to a solution of *p*-cresol **1** (18 mM) in CH_2Cl_2 (2.5 mL) containing the opportune amount of buffer (275 μL). The initial rates of the reaction were measured by means of the same procedure described for the determination of the kinetic constants. Each sample was assessed in triplicate, and the tyrosinase activity was expressed as the relative percentage activity with respect to that at time zero.

Enzyme Recycling. The reusability of catalysts **I** and **IV** in aqueous medium was determined by recording the time-dependent increase in absorbance at 475 nm (dopachrome formation) during L-tyrosine oxidation. The catalyst was then recovered by centrifugation, washed to remove the substrate, and reused again. The reusability of catalysts **I** and **IV** in the organic solvent was determined by measuring the initial rates of the reaction with the substrate at 25 °C. Briefly, 5.0 mg of *p*-cresol **1**, 1.0 mg of **I** or **IV**, 275 μL of buffer, and 2.5 mL of CH_2Cl_2 were placed in a flask at 25 °C under O_2. The reaction mixture was vigorously shaken, and the initial rates of the reaction were measured by means of the same procedure described for the determination of the kinetic constants. After 30 min, the catalyst was recovered in the aqueous solution by phase separation, centrifuged, washed to remove the substrate, and reused again. For each run, the tyrosinase activity was expressed as the relative percentage activity with respect to that of the first run.

Oxidation of Phenols. The oxidation of phenols **1**–**5** in the biphasic CH_2Cl_2/buffer system was performed following a procedure previously optimized by our group.[25] Briefly, to a solution of the substrate (0.05 mmol) in CH_2Cl_2 (2.5 mL) was added the opportune amount of native or immobilized tyrosinase (240 units) in PBS (275 μL), and the mixture was stirred at room

dx.doi.org/10.1021/cs400856e | ACS Catal. 2014, 4, 810–822

temperature under O_2. Reactions were monitored by thin layer chromatography (TLC). After 24 h, the two phases were separated by decantation, and in the case of immobilized tyrosinase, the catalyst was recovered by centrifugation of the aqueous layer. The organic fraction was concentrated with a rotary evaporator and taken up with a solution of sodium dithionite in THF and H_2O [1:1 (v/v)]. The mixture was stirred at room temperature for 5 min to allow the complete reduction of benzoquinones to catechols and extracted twice with ethyl acetate. The collected organic extracts were dried over anhydrous sodium sulfate, filtered, and concentrated under vacuum. For gas chromatography and mass spectrometry (GC−MS), the residue was treated with anhydrous pyridine (kept over NaOH pellets) and a 2:1 HMDS/TMCS mixture under vigorous stirring at room temperature for 30 min and then allowed to stand for 5 min.[36] Dodecane (1 μL) was used as an internal standard. The oxidation of **1** in buffer was performed following a previously reported protocol.[5] In a general procedure, a solution of **1** (0.05 mmol), ascorbic acid (1.5 equiv), and the appropriate amount of native or immobilized tyrosinase (240 units) in 0.1 M PBS (pH 7.0, 5.0 mL) were stirred at 25 °C under O_2. The reactions were monitored by TLC. After the disappearance of the substrate, the mixture was acidified with a solution of 1.0 M HCl and extracted twice with EtOAc. In the case of immobilized tyrosinase, the biocatalyst was first removed from the reaction mixture by centrifugation. The collected organic extracts were washed with a saturated solution of NaCl, dried over anhydrous Na_2SO_4, filtered, and concentrated. The obtained colored residue was analyzed by GC−MS as previously reported. All experiments were conducted in triplicate.

■ ASSOCIATED CONTENT

Supporting Information

Relationship diagram between absorbance and the concentration of oxidized carbon nanotubes (ox-MWCNTs), plots of activity (percent) of catalysts **I** and **IV** versus run in buffer and in organic medium, linear regression equations and plots of Lineweaver−Burk, Eadie−Hofstee, and Hanes analyses for native tyrosinase and catalyst **I**, nonlinear regression plot for native tyrosinase and catalyst **I**, and data for the identification and characterization of the oxidation products. This material is available free of charge via the Internet at http://pubs.acs.org.

■ AUTHOR INFORMATION

Corresponding Authors

*E-mail: marcello.crucianelli@univaq.it. Fax: (+39) 0862-433753.

*E-mail: saladino@unitus.it. Fax: (+39) 0761-357242.

Notes

The authors declare no competing financial interest.

■ ACKNOWLEDGMENTS

F.S. thanks the University of L'Aquila for a research grant. The Italian Space Agency (ISA) is greatly acknowledged for its financial support.

■ REFERENCES

(1) For selected recent reviews on this general topic, see: (a) Brena, B.; González-Pombo, P.; Batista-Viera, F. *Methods Mol. Biol.* **2013**, *1051*, 15−31. (b) Barbosa, O.; Torres, R.; Ortiz, C.; Berenguer-Murcia, A.; Rodrigues, R. C.; Fernandez-Lafuente, R. *Biomacromolecules* **2013**, *14*, 2433−2462. (c) Rodrigues, R. C.; Ortiz, C.; Berenguer-Murcia, A.; Torres, R.; Fernández-Lafuente, R. *Chem. Soc. Rev.* **2013**, *42*, 6290−6307. (d) Zhou, Z.; Hartmann, M. *Chem. Soc. Rev.* **2013**, *42*, 3894−3912. (e) Verma, M. L.; Barrow, C. J.; Puri, M. *Appl. Microbiol. Biotechnol.* **2013**, *97*, 23−39. (f) Hwang, E. T.; Gu, M. B. *Eng. Life Sci.* **2013**, *13*, 49−61. (g) Rajkumar, K.; Palla, S.; Paladugu, A.; Reddy, E. R.; Reddy, K. R. *Int. Res. J. Pharm.* **2013**, *4*, 36−44. (h) Tran, D. N.; Balkus, K. J., Jr. *ACS Catal.* **2011**, *1*, 956−968. (i) Garcia-Galan, C.; Berenguer-Murcia, A.; Fernandez-Lafuente, R.; Rodrigues, R. C. *Adv. Synth. Catal.* **2011**, *353*, 2885−2904.

(2) (a) Seo, S.-Y.; Sharma, V. K.; Sharma, N. *J. Agric. Food Chem.* **2003**, *51*, 2837−2853. (b) Halaouli, S.; Asther, M.; Sigoillot, J.-C.; Hamdi, M.; Lomascolo, A. *J. Appl. Microbiol.* **2006**, *100*, 219−232.

(3) (a) Duran, N.; Rosa, M. A.; D'Annibale, A.; Gianfreda, L. *Enzyme Microb. Technol.* **2002**, *31*, 907−931. (b) Munjal, N.; Sawhney, S. K. *Enzyme Microb. Technol.* **2002**, *30*, 613−619. (c) Sanz, V. C.; Mena, M. L.; Gonzalez-Cortes, A.; Yanez-Sedeno, P.; Pingarron, J. M. *Anal. Chim. Acta* **2005**, *528*, 1−8. (d) Arslan, A.; Kiralp, S.; Toppare, L.; Yagci, Y. *Int. J. Biol. Macromol.* **2005**, *35*, 163−167. (e) Jaafar, A.; Musa, A.; Nadarajah, K.; Lee, Y. H.; Hamidah, S. *Sens. Actuators, B* **2006**, *114*, 604−609. (f) Zejli, H.; Hidalgo-Hidalgo de Cisneros, J. L.; Naranjo-Rodriguez, I.; Liu, B.; Temsamani, K. R.; Marty, J. L. *Anal. Chim. Acta* **2008**, *612*, 198−203. (g) Fiorentino, D.; Gallone, A.; Fiocco, D.; Palazzo, G.; Mallardi, A. *Biosens. Bioelectron.* **2010**, *25*, 2033−2037. (h) Dinçer, A.; Becerik, S.; Aydemir, T. *Int. J. Biol. Macromol.* **2012**, *50*, 815−820.

(4) (a) Thalmann, C. R.; Lötzbeyer, T. *Eur. Food Res. Technol.* **2002**, *214*, 276−281. (b) Chen, T.; Embree, H. D.; Wu, L. Q.; Payne, G. F. *Biopolymers* **2002**, *64*, 292−302. (c) Huang, T. H.; Kuwana, T.; Warsinke, A. *Biosens. Bioelectron.* **2002**, *17*, 1107−1113. (d) Anghileri, A.; Lantto, R.; Kruus, K.; Arosio, C.; Freddi, G. *J. Biotechnol.* **2007**, *127*, 508−519. (e) Marìn-Zamora, M. E.; Rojas-Melgarejo, F.; García-Cánovas, F.; García-Ruiz, P. A. *J. Biotechnol.* **2009**, *139*, 163−168. (f) Tuncagil, S.; Kayahan, S. K.; Bayramoglu, G.; Arica, M. Y.; Toppare, L. *J. Mol. Catal. B: Enzym.* **2009**, *58*, 187−193. (g) Hanifah, S. A.; Heng, L. Y.; Ahmad, M. *Anal. Sci.* **2009**, *25*, 779−784. (h) Yin, H.; Zhou, Y.; Xu, J.; Ai, S.; Cui, L.; Zhu, L. *Anal. Chim. Acta* **2010**, *659*, 144−150. (i) Donato, L.; Algieri, C.; Miriello, V.; Mazzei, R.; Clarizia, G.; Giorno, L. *J. Membr. Sci.* **2012**, *407*, 86−92.

(5) Guazzaroni, M.; Crestini, C.; Saladino, R. *Bioorg. Med. Chem.* **2012**, *20*, 157−166.

(6) Feng, W.; Ji, P. *Biotechnol. Adv.* **2011**, *29*, 889−895.

(7) Apetrei, I. M.; Rodriguez-Mendez, M. L.; Apetrei, C.; de Saja, J. A. *Sens. Actuators, B* **2013**, *177*, 138−144.

(8) (a) Kong, L.; Huang, S.; Yue, Z.; Peng, B.; Li, M.; Zhang, J. *Microchim. Acta* **2009**, *165*, 203−209. (b) Yina, H.; Zhoua, Y.; Xua, J.; Aia, S.; Cuia, L.; Zhub, L. *Anal. Chim. Acta* **2010**, *659*, 144−150. (c) Hashemnia, S.; Khayatzadeh, S.; Hashemnia, M. *J. Solid State Electrochem.* **2012**, *16*, 473−479.

(9) Romão Sartori, E.; Campanhã Vicentinia, F.; Fatibello-Filho, O. *Talanta* **2011**, *87*, 235−242.

(10) (a) Decher, G.; Schmitt, J. *Prog. Colloid Polym. Sci.* **1992**, *89*, 160−164. (b) Decher, G. *Science* **1997**, *277*, 1232−1237.

(11) (a) Mateo, C.; Fernandes, B.; Van Rantwijk, F.; Stolz, A.; Sheldon, R. A. *J. Mol. Catal. B: Enzym.* **2006**, *38*, 154−157. (b) Wilson, L.; Illanes, A.; Abián, O.; Pessela, B. C. C.; Fernández-Lafuente, R.; Guisán, J. M. *Biomacromolecules* **2004**, *5*, 852−857. (c) Abián, O.; Wilson, L.; Mateo, C.; Fernández-Lorente, G.; Palomo, J. M.; Fernández-Lafuente, R.; Guisán, J. M.; Re, D.; Tam, A.; Daminatti, M. *J. Mol. Catal. B: Enzym.* **2002**, *19*−*20*, 295−303. (d) Abián, O.; Mateo, C.; Fernández-Lorente, G.; Palomo, J. M.; Fernández-Lafuente, R.; Guisán, J. M. *Biocatal. Biotransform.* **2001**, *19*, 489−503. (e) Barbosa, O.; Ortiz, C.; Berenguer-Murcia, A.; Torres, R.; Rodrigues, R. C.; Fernandez-Lafuente, R. *RSC Adv.* **2014**, *4*, 1583−1600. (f) Shah, S.; Sharma, A.; Gupta, M. N. *Anal. Biochem.* **2006**, *351*, 207−213.

(12) Asuri, P.; Karajanagi, S. S.; Sellitto, E.; Kim, D.-Y.; Kane, R. S.; Dordick, J. S. *Biotechnol. Bioeng.* **2006**, *95*, 804−811.

(13) Robb, D. A.; Gutteridge, S. *Phytochemistry* **1981**, *20*, 1481−1485.

(14) (a) Iamsamai, C.; Soottitantawat, A.; Ruktanonchai, U.; Hannongbua, S.; Dubas, S. T. *Carbon* **2011**, *49*, 2039−2045. (b) Lee, J.; Park, S.-J.; Moon, Y.-K.; Kim, S.-H.; Koh, K. *Korean J. Chem. Eng.* **2009**, *26*, 1790−1794.

(15) Xiang, Y.; Zhang, Y.; Jiang, B.; Chai, Y.; Yuan, R. *Sens. Actuators, B* **2011**, *155*, 317−322.
(16) Ziółkowska, D.; Shyichuk, A.; Zelazko, K. *Polimery* **2012**, *57*, 303−305.
(17) Masamoto, Y.; Iida, S.; Kubo, M. *Planta Med.* **1980**, *40*, 361−365.
(18) (a) Martın, M. T.; Plou, F. J.; Alcalde, M.; Ballesteros, A. *J. Mol. Catal. B: Enzym.* **2003**, *21*, 299−308. (b) Knezevic, Z.; Milosavic, N.; Bezbradica, D.; Jakovljevic, Z.; Prodanovic, R. *Biochem. Eng. J.* **2006**, *30*, 269−278.
(19) Gao, Y.; Kyratzis, I. *Bioconjugate Chem.* **2008**, *19*, 1945−1950.
(20) Yu, C.-M.; Yen, M.-J.; Chen, L.-C. *Biosens. Bioelectron.* **2010**, *25*, 2515−2521.
(21) Shah, S.; Solanki, K.; Gupta, M. N. *Chem. Cent. J.* **2007**, *1*, 30−36.
(22) (a) Piao, Y.; Jin, Z.; Lee, D.; Lee, H.-J.; Na, H.-B.; Hyeon, T.; Oh, M.-K.; Kim, J.; Kim, H.-S. *Biosens. Bioelectron.* **2011**, *26*, 3192−3199. (b) Ren, J.; Kang, T.-F.; Xue, R.; Ge, C.-N.; Cheng, S.-Y. *Microchim. Acta* **2011**, *174*, 303−309.
(23) Horcas, I.; Fernández, R.; Gómez-Rodríguez, J. M.; Colchero, J.; Gómez-Herrero, J.; Baro, A. M. *Rev. Sci. Instrum.* **2007**, *78*, 013705/1−013705/8.
(24) (a) Kazandjiand, R. A.; Klibanov, M. *J. Am. Chem. Soc.* **1985**, *107*, 5448−5450. (b) Kermasha, S.; Tse, M. *J. Chem. Technol. Biotechnol.* **2000**, *75*, 475−483. (c) Kermasha, S.; Bao, H.; Bisakowski, B.; Yaylayan, V. *J. Mol. Catal. B: Enzym.* **2001**, *11*, 929−938. (d) Kermasha, S.; Bao, H.; Bisakowski, B. *J. Mol. Catal. B: Enzym.* **2002**, *19*, 335−345.
(25) Guazzaroni, M.; Pasqualini, M.; Botta, G.; Saladino, R. *ChemCatChem* **2012**, *4*, 89−99.
(26) Torchilin, V. P.; Maksimenko, A. V.; Smirnov, V. N.; Berezin, I. V.; Klibanov, A. M.; Martinek, K. *Biochim. Biophys. Acta* **1978**, *522*, 277−283.
(27) Aytar, B. S.; Bakir, U. *Process Biochem. (Oxford, U.K.)* **2008**, *43*, 125−131.
(28) (a) Ren, L.; Zhong, W. *Environ. Sci. Technol.* **2010**, *44*, 6954−6958. (b) Ren, L.; Yan, D.; Zhong, W. *Carbon* **2012**, *50*, 1303−1310.
(29) (a) Zheng, L. T.; Ryu, G. M.; Kwon, B. M.; Lee, W. H.; Suk, K. *Eur. J. Pharmacol.* **2008**, *588*, 106−113. (b) Nolan, L. C.; O'Connor, K. E. *Biotechnol. Lett.* **2008**, *30*, 1879−1891. (c) Shimizu, T.; Nakanishi, Y.; Nakahara, M.; Wada, N.; Moro-Oka, Y.; Hirano, T.; Konishi, T.; Matsugo, S. *J. Clin. Biochem. Nutr.* **2010**, *47*, 181−190.
(30) (a) Carvalho, G. M. J.; Alves, T. L. M.; Freire, D. M. G. *Appl. Biochem. Biotechnol.* **2000**, *84*, 791−800. (b) Ullrich, R.; Hofrichter, M. *Cell. Mol. Life Sci.* **2007**, *64*, 271−293. (c) Otavio de Faria, R.; Rotuno-Moure, V.; Lopes deAlmeida, M. A.; Krieger, N.; Mitchell, D. A. *Food Technol. Biotechnol.* **2007**, *45*, 287−294.
(31) Burton, S. G.; Duncan, J. R.; Kaye, P. T.; Rose, P. D. *Biotechnol. Bioeng.* **1993**, *42*, 938−944.
(32) Da Silva, A. M.; Junqueira, G. M. A.; Anconi, C. P. A.; Dos Santos, H. F. *J. Phys. Chem. C* **2009**, *113*, 10079−10084.
(33) Ismaya, W. T.; Rozeboom, H. J.; Schurink, M.; Boeriu, C. G.; Wichers, H.; Dijkstra, B. W. *Acta Crystallogr.* **2011**, *F67*, 575−578.
(34) (a) Bradford, M. M. *Anal. Biochem.* **1976**, *72*, 248. (b) Sedmak, J. J.; Grossberg, S. E. *Anal. Biochem.* **1977**, *79*, 544−552.
(35) Bi, S.; Zhou, H.; Zhang, S. *Biosens. Bioelectron.* **2009**, *24*, 2961−2966.
(36) (a) Sweely, C. C.; Bentlry, R.; Makita, M.; Wells, W. W. *J. Am. Chem. Soc.* **1963**, *85*, 2497−2507. (b) Rodríguez-López, J. N.; Gómez-Fenoll, L.; Penalver, M. J.; García-Ruíz, P. A.; Varón, V.; Martínez-Ortíz, F.; García-Cánovas, F.; Tudela, J. *Biochim. Biophys. Acta* **2001**, *1548*, 238−256.